KOPIO Technical Note 131

A Fit to the Kp2 Odd Background Hypothesis

Paolo Rumerio, Stony Brook

March 22, 2005

Abstract

A fitter to the kp2 odd background hypothesis has been developed.

1 Introduction

The FASTMC is used to generate kp2 events which are labeled as

$$K_L^0 \to \pi_1^0\pi_2^0 \; ; \; \pi_1^0 \to \gamma_1\gamma_3 \; , \; \pi_2^0 \to \gamma_2\gamma_4 \; , \tag{1}$$

Photons γ_1 and γ_2 are treated as converted in the preradiator (PR) and information on their energy, direction, detection position and time are used. Photons γ_3 and γ_4 are assumed undetected.

From the measurement of γ_1 and γ_2, and by assuming a kp2-odd kinematics, the energy and direction of γ_3 and γ_4 can be determined with a 2-fold ambiguity. The procedure is as follows.

1. The K_L^0 decay vertex is determined from the measured directions of γ_1 and γ_2 (the y-dimension of the beam will also be used by the kp2-odd fitter).

2. By assuming that the K_L^0 was generated at the center of the target and at the "central" time of the microbunch, the K_L^0 momentum is calculated through its time of flight.

3. A boost from Lab to K_L^0 center of mass (CM) system is performed. Fig. 1 is a representation of the CM momentum of the particles in the decay $\pi_1^0 \to \gamma_1\gamma_3$. All variables used below and in Fig. 1 are understood in the CM system.

4. In the CM system, the known energy of the π^0's, $E_\pi = m_K/2$, and the measured energy of γ_1, E_{γ_1}, allow us to calculate the energy of γ_3, $E_{\gamma_3} = E_\pi - E_{\gamma_1}$, and the opening angle between γ_1 and γ_3,

$$\cos\alpha_1 = 1 - \frac{m_\pi^2}{2E_{\gamma_3}E_{\gamma_1}} \ . \tag{2}$$

The angle between γ_1 and π_1 is calculated as

$$\cos\delta_1 = \frac{E_{\gamma_1} + E_{\gamma_3}\cos\alpha_1}{P_\pi} \ , \tag{3}$$

where $P_\pi = \sqrt{E_\pi^2 - m_\pi^2} = 209.05$ MeV.

5. We can then affirm that the momentum of π_1 lies on a cone of opening angle δ_1 about the direction of γ_1, as shown in Fig. 1. In a rotated CM system, $x'y'z'$, where the z'-axis is in the direction of γ_1, the possible values of the momentum of π_1 can be parameterized as

$$\begin{cases} P_{\pi_1,x'} = P_\pi \ \sin\delta_1 \ \cos\omega_1 \\ P_{\pi_1,y'} = P_\pi \ \sin\delta_1 \ \sin\omega_1 \\ P_{\pi_1,z'} = P_\pi \ \cos\delta_1, \end{cases} \tag{4}$$

where ω_1 will be an unmeasured parameter of the kp2-odd fitter.

6. The system xyz can be transformed into $x'y'z'$ by means of the 2 rotations indicated in Fig. 1 (the freedom of defining the axis x' spares a third rotation). In the original system xyz, the momentum of π_1 is

$$\begin{cases} P_{\pi_1,x} = +P_{\pi_1,x'} \ \cos\theta_1 \ \cos\phi_1 - P_{\pi_1,y'} \ \sin\phi_1 - P_{\pi_1,z'} \ \sin\theta_1 \ \cos\phi_1 \\ P_{\pi_1,y} = +P_{\pi_1,x'} \ \cos\theta_1 \ \sin\phi_1 + P_{\pi_1,y'} \ \cos\phi_1 + P_{\pi_1,z'} \ \sin\theta_1 \ \sin\phi_1 \\ P_{\pi_1,z} = -P_{\pi_1,x'} \ \sin\theta_1 + P_{\pi_1,z'} \ \cos\theta_1 \end{cases} \tag{5}$$

7. By inserting Eqs. 4 into Eqs. 5, we obtain a parameterization of the π_1 momentum in the system xyz (i.e. the original CM system) in terms of measured quantities and a single new parameter ω_1 .

8. In the same way, we can write the momentum of π_2 in the system xyz in terms of measured quantities and another unmeasured parameter ω_2.

9. We now have equations for both π_1 and π_2 momenta in the same reference system, xyz, and can require total momentum conservation. Since Eqs. 5 and 4 automatically guarantee that the magnitude of the momenta of π_1 and π_2 is equal to $P_\pi = 209.05$ MeV, it is sufficient to require that the directions of π_1 and π_2 are opposite to eachother. The CM polar and azimuthal angles, ϕ_{π_i} and θ_{π_i}, of the pions can be calculated from Eqs. 5 to impose 2 constraints,
$$\begin{cases} |\phi_{\pi_1} - \phi_{\pi_2}| - \pi = 0 \\ \theta_{\pi_1} + \theta_{\pi_2} - \pi = 0, \end{cases} \tag{6}$$
that are functions of the 2 newly introduced unmeasured parameters ω_1 and ω_2.

In general, the kinematic problem of the kp2-odd has 2 distinct solutions for the momentum of the unmeasured photons. Fig. 2 and its caption help in visualizing this fact.

Given one of the 2 solutions, say 1st solution, the second one is calculated as follows. Referring to Fig. 2, the unity vector that points from the 1st to the 2nd solution for $\vec{P}_{\pi_1}$ is
$$\vec{u}_T = \frac{\vec{P}_1 \times \vec{P}_2}{|\vec{P}_1 \times \vec{P}_2|}. \tag{7}$$
The momentum that has to be added to the available solution to obtain the alternative one is
$$\vec{P}_T = -2\,[\vec{P}_{\pi_1}(\text{1st solut.}) \cdot \vec{u}_T]\,\vec{u}_T, \tag{8}$$
and therefore
$$\vec{P}_{\pi_1}(\text{2nd solut.}) = \vec{P}_{\pi_1}(\text{1st solut.}) + \vec{P}_T. \tag{9}$$
The procedure works without modification independently from which of the 2 solutions of Fig. 2 is assumed to be available.

The 2 solutions are not distinguishable by the KOPIO apparatus, as they share the same values for the quantities of γ_1, γ_2 and K_L^0. The 2 solutions differ only in the values of the quantities of the unmeasured photons, γ_3 and γ_4 (and obviously of the 2 pions and ω_1 and ω_2).

2 The kp2-odd fitter

The kp2-odd fitting routine is given 15 measured and 5 unmeasured variables. The measured ones are the energy, the detection time, the 3 detection positions and the

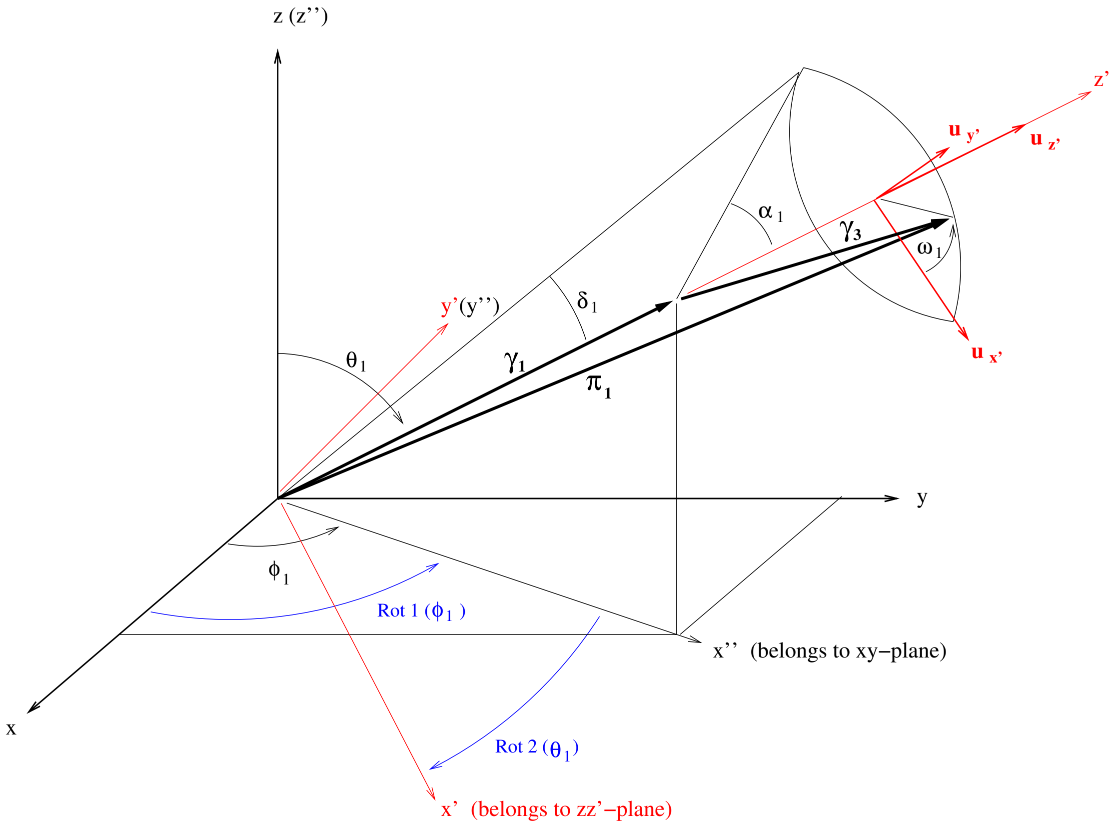

Figure 1: The momentum of the particles $\pi_1^0 \to \gamma_1\gamma_3$ in the K_L^0 CM system xyz. The polar and azimuthal angles of the momentum of γ_1 are ϕ_1 and θ_1. The system xyz can be transformed into an intermediate system $x''y''z''$ by a rotation of an angle ϕ_1 about z. The system $x''y''z''$ is then rotated of an angle θ_1 about y'' into a system $x'y'z'$ which has the z'-axis along the direction of γ_1 and the x'-axis in the zz'-plane. In the system $x'y'z'$ (unity vectors $\vec{u}_{x'}$, $\vec{u}_{y'}$ and $\vec{u}_{x'}$), the possible values of the momentum of π_1 are easily parameterized by Eqs. 4.

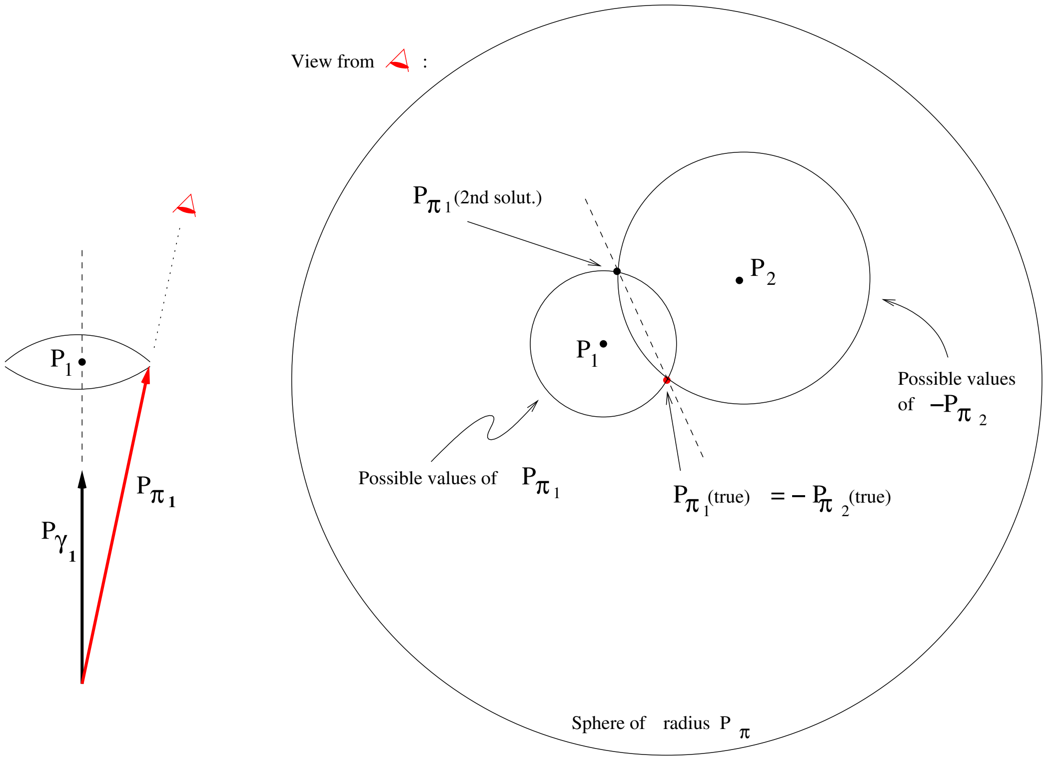

Figure 2: Left: a sketch of the true CM momenta of γ_1, $\vec{P}_{\gamma_1}$, and π_1, $\vec{P}_{\pi_1}$, as well as a circle representing the possible values of $\vec{P}_{\pi_1}$. Right: a view of this sketch by looking into the direction of the true $\vec{P}_{\pi_1}$ (the red dot). The circle of possible values of $\vec{P}_{\pi_1}$ lies on a sphere of radius $P_\pi = \sqrt{(m_K/2)^2 - m_\pi^2}$. The point P_1 is the intersection point between the continuation of $\vec{P}_{\gamma_1}$ and the sphere (P_1 can also be seen as the end point of a vector $\vec{P}_1 \equiv \vec{P}_{\gamma_1} \times P_\pi/E_{\gamma_1}$). The point P_2 is the intersection between the continuation of $-\vec{P}_{\gamma_2}$ and the sphere (also seen as the end point of a vector $\vec{P}_2 \equiv -\vec{P}_{\gamma_2} \times P_\pi/E_{\gamma_2}$). The possible values of $-\vec{P}_{\pi_2}$ also describe a circle that lies on the sphere of radius P_π. Since the true value of $\vec{P}_{\pi_1}$ is equal to the true value of $-\vec{P}_{\pi_2}$, the 2 circles of possible values of $\vec{P}_{\pi_1}$ and $-\vec{P}_{\pi_2}$ intersect at the red dot. In general, a second intersection between the 2 circles exist, producing a second solution to the kinematic problem of the kp2-odd background.

It should be noticed that if the event is a kp2-even event, then $\vec{P}_1$, $\vec{P}_2$ and $\vec{P}_{\pi_1}$ are coplanar and only one intersection exists.

2 directions of each of the measured photons; and the y-position of the K_L^0 decay vertex assumed to be within the beam y-dimension. The first 3 unmeasured variables are the x- and z-position, and the time of the K_L^0 decay. The variables listed above are the same ones used by the fit to the $X \to \gamma_1\gamma_2$ hypothesis in the standard FASTMC code (usually called Fit 1, as opposite to Fit 2 which adds the constraint $m_X = m_{\pi^0}$). The 2 additional unmeasured variables given to the kp2-odd fitter are the previously described ω_1 and ω_2. The number of constraints of the kp2-odd fitter is 8. The first 6 constraints are the same ones used by the fitter to $X \to \gamma_1\gamma_2$, that is the time and 2 directions of each of the measured photons. The 2 additional constraints in Eqs. 6 are necessary to force total momentum conservation[1].

The measured variables and their uncertainties are passed to the kp2-odd fitter. Initial values for the unmeasured variables of the K_L^0 decay vertex and time are calculated using the method of the distance of closest approach between the trajectories of γ_1 and γ_2. In order to obtain initial values for ω_1 and ω_2, the first step is to calculate analytical solutions for the CM momentum of the unmeasured photons, γ_3 and γ_4. This is done by Dima Vavilov's routine KINGPS. Hence, the CM momenta of γ_3 and γ_4 are used to calculate the CM momenta of π_1 and π_2. The latter two are then projected on the unity vectors $\vec{u}_{x'}$ and $\vec{u}_{y'}$ as described in

[1]However, it is empirically observed that using the constraints in Eqs. 6 the percentage of convergence of the kp2-odd fitter applied to kp2-odd events is only $\sim 62\%$. If the 3 constraints

$$\begin{cases} P_{\pi_1,x} + P_{\pi_2,x} = 0 \\ P_{\pi_1,y} + P_{\pi_2,y} = 0 \\ P_{\pi_1,z} + P_{\pi_2,z} = 0, \end{cases} \tag{10}$$

are used instead, the percentage of convergence increases to $\sim 90\%$. Although the latter is not the correct form for imposing the constraints (which should be only 2: the magnitude of the momenta of the pions is fixed; therefore, once the first two of Eqs. 10 are satisfied, the third one only resolves a sign ambiguity between $P_{\pi_1,z}$ and $P_{\pi_2,z}$) the code currently implements Eqs. 10 given the higher percentage of convergence. To the purpose of calculating the probability of χ^2, only 2 constraints are counted.

footnote [2]. (A technical note: the kp2-odd reconstruction code can also be run without performing the kp2-odd fit. In this case, the results of the fit to $X \to \gamma_1\gamma_2$ are used for the γ_1 and γ_2 momenta and the K_L^0 decay vertex and time; and the routine KINGPS is called to calculate the analytical solutions for γ_3 and γ_4.)

The kp2-odd fitter varies the measured and unmeasured variables in the Lab system (only ω_1 and ω_2 are CM variables), performs steps 1 through 9 in the Introduction section to calculate and impose the constraints, and find a solution of the minimization problem. A second solution is found using Eqs. 7-9, leaving unchanged the fit results for all measured variables and K_L^0 decay vertex and time. The only quantities that are changed are the momenta of pions and unmeasured photons (and of course the unmeasured variables ω_1 and ω_2).

3 Fitter efficiency and resolution

The kp2-odd fit converges for about 90% of the kp2-odd events with γ_1 and γ_2 in the preradiator. An error code, `OddIerr`, is set = 0 for normal fit convergence. For 5% of the events the fitter exceeds the maximum number of iteration, in this study increased to 50 from the current usual value 20 (`OddIerr` = 2). For the remaining 5% of the events the fit fails. A failure generally happens when the fitter moves the LAB variables to unphysical values (e.g. LAB values that determine a CM energy of γ_1 or $\gamma_2 < 19.9$ MeV or > 228.9 MeV) and is not able to recover (`OddIerr` = 7). (More to be said on this point.) Events with `OddIerr` = 2 are in principle recoverable at the expenses of a longer processing time. Events with

[2] According to the value of a determinant that can be $>$, $=$ or < 0, KINGPS returns 2, 1 or 0 solutions for the CM momenta of γ_3 and γ_4. The 3 possibilities correspond to intersecting, tangent or non-intersecting circles in Fig. 2. If KINGPS returns 2 solutions (tangent circles is virtually impossible) the 1st analytical solutions for γ_3 and γ_4 is used to calculate the CM momentum, $\vec{P}_{\pi_1}$ and $\vec{P}_{\pi_2}$, of π_1 and π_2. Focusing on π_1 (π_2 is done analogously), the initial value for ω_1 is calculated using

$$\cos\omega_1 = \frac{\vec{P}_{\pi_1,x'y'}}{|\vec{P}_{\pi_1,x'y'}|} \cdot \vec{u}_{x'} \quad \text{and} \quad \sin\omega_1 = \frac{\vec{P}_{\pi_1,x'y'}}{|\vec{P}_{\pi_1,x'y'}|} \cdot \vec{u}_{y'} \;, \tag{11}$$

where $\vec{P}_{\pi_1,x'y'} \equiv \vec{P}_{\pi_1} - \vec{u}_{z'}\,(\vec{P}_{\pi_1} \cdot \vec{u}_{z'})$ is the component of $\vec{P}_{\pi_1}$ on the $x'y'$-plane. The unity vectors $\vec{u}_{x'}$, $\vec{u}_{y'}$ and $\vec{u}_{z'}$ are shown in red in Fig. 1 and are calculated by

$$\vec{u}_{z'} \equiv \vec{P}_{\gamma_1}/|\vec{P}_{\gamma_1}| \,, \quad \vec{u}_{y'} \equiv \vec{u}_z \times \vec{u}_{z'}/|\vec{u}_z \times \vec{u}_{z'}| \;\; [\vec{u}_z \equiv (0,0,1)] \quad \text{and} \quad \vec{u}_{x'} \equiv \vec{u}_{y'} \times \vec{u}_{z'} \;. \tag{12}$$

`OddIerr` = 7 could be recoverable although attempts made so far have not been successful.

For the kp2-odd events with a converging kp2-odd fit, the plots in Fig.s 3, 4, 5 and 6 show a comparison between the fit results and the true value of the 4-momentum of the undetected photon γ_3. Analogous plots can be made for γ_4. In Fig.s 3 and 5, a "best solution" among the 2 available ones is defined as the one that minimizes

$$\left[\vec{P}_{\gamma_3}(i^{th}\ \text{solut.}) - \vec{P}_{\gamma_3}(\text{true})\right]^2 + \left[\vec{P}_{\gamma_4}(i^{th}\ \text{solut.}) - \vec{P}_{\gamma_4}(\text{true})\right]^2$$

where i^{th} solut. is the 1st or 2nd solution. As already mentioned, with real data there will not be any criteria to determine which one of the 2 solutions is the closest to the truth.

For each undetected photon, Fig. 7 shows the angle, $\Delta\psi$, between the predicted and true direction. $\Delta\psi$ is calculated by

$$\Delta\psi = \arccos\left(\frac{\vec{P}_{\gamma/\text{pred}} \cdot \vec{P}_{\gamma/\text{true}}}{E_{\gamma/\text{pred}}\, E_{\gamma/\text{true}}}\right). \tag{13}$$

The kp2-odd fitter resolution for the momenta of the unmeasured photons γ_3 and γ_4 is similar to the resolution obtained by calculating the analytical solutions of the kp2-odd kinematic problem. On the other hand, the kp2-odd fitter recovers most of those kp2-odd events for which the analytical solutions do not exist (the numbers are in table 1 in next section). The resolution of the kp2-odd fitter on the reconstructed vertex of the K^0 is similar to the resolution of the fit to the hypothesis $X \to \gamma_1\gamma_2$, as shown in Fig. 8.

To campare the resolution of the kp2-odd fitter for events with and without analytical solutions of the kp2-odd kinematic problem, Figs. 9 and 10 are added.

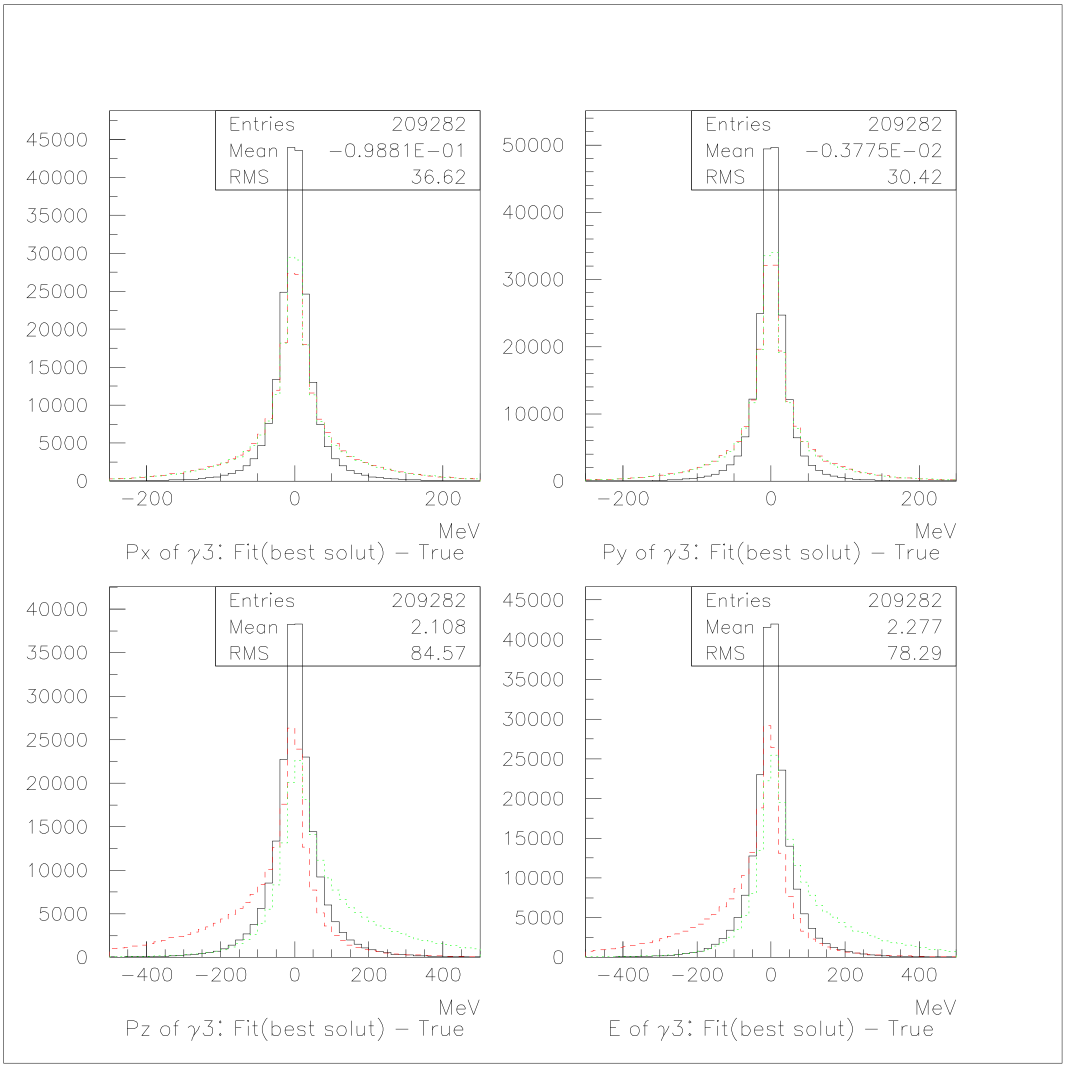

Figure 3: Difference between the fit results for the LAB 4-momentum of γ_3 and the corresponding true values. In each plot, the solid histograms represent the best one of the 2 possible solutions. However, the information on which one is the best solution will not be available with real data. The 2 dashed histograms of each plot represent the 1st and 2nd solutions separately.

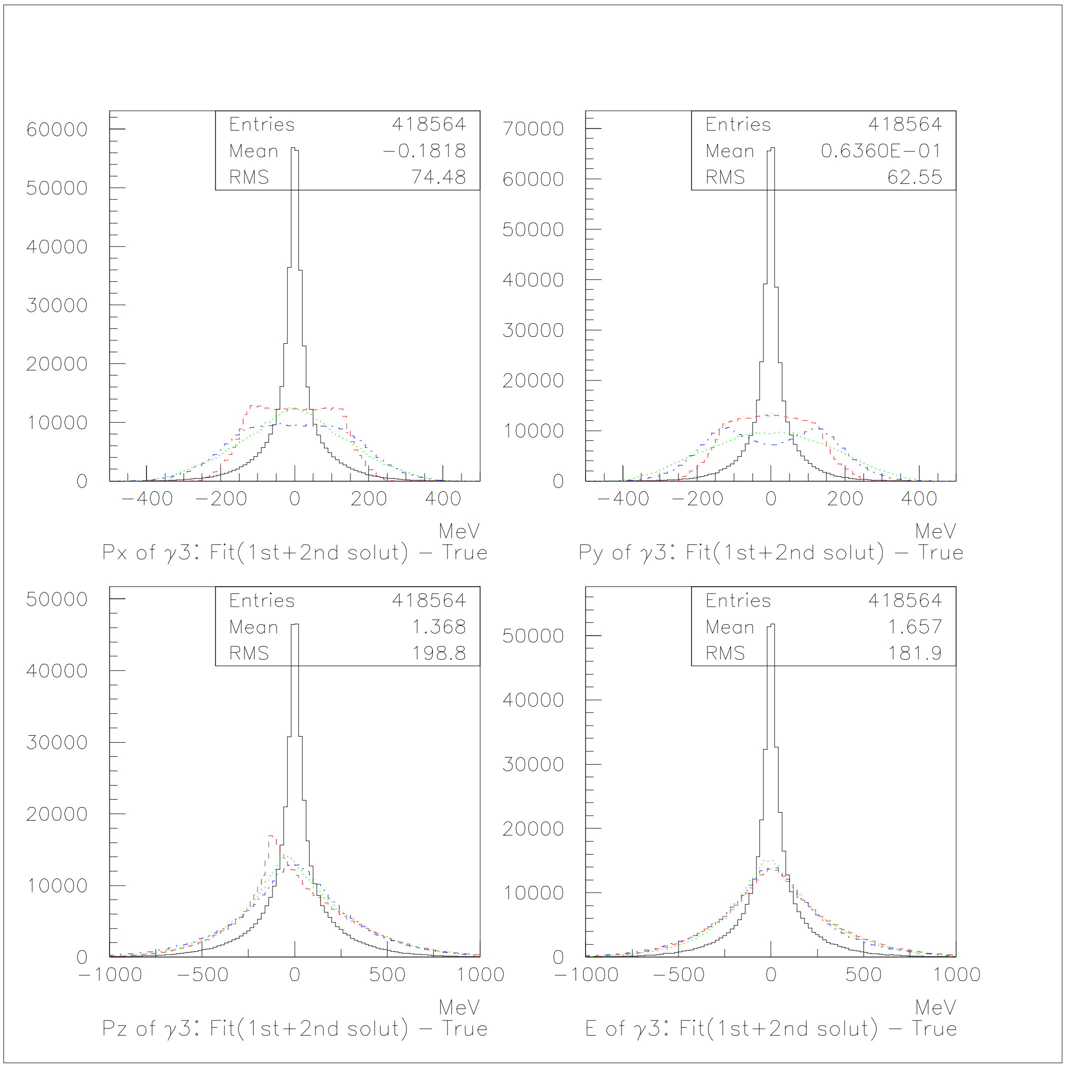

Figure 4: As opposite to Fig. 3, here the solid histogram contains both the 1st and 2nd solutions as we will not be able to establish which is the best one with real data. As a test, in the dashed histograms the true values of the 4-momentum of γ_3 have been replaced with the true values of the 4-momentum of γ_4, γ_1 and γ_2.

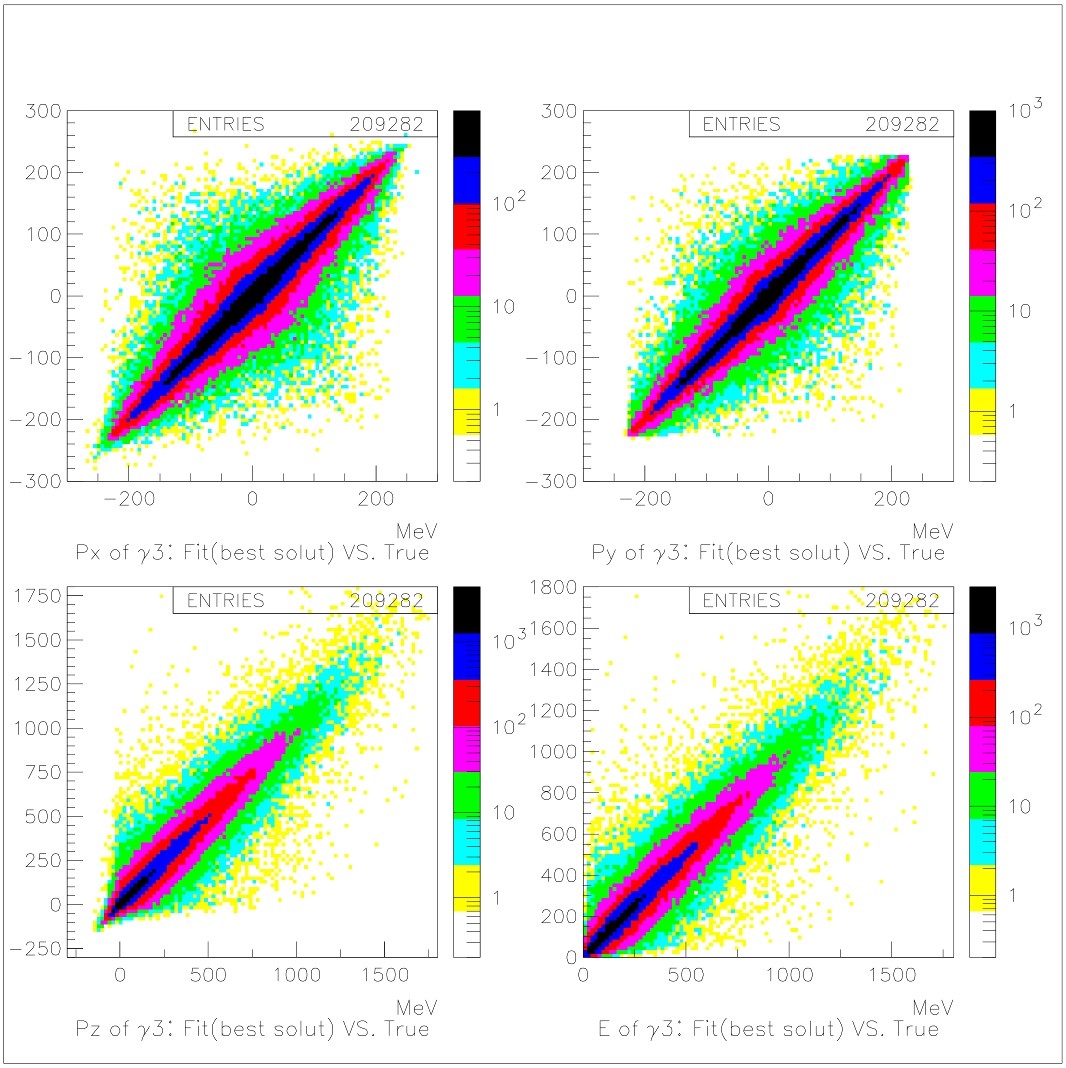

Figure 5: The fit results for the LAB 4-momentum of γ_3 versus the corresponding true values. The best one of the 2 possible solutions is used.

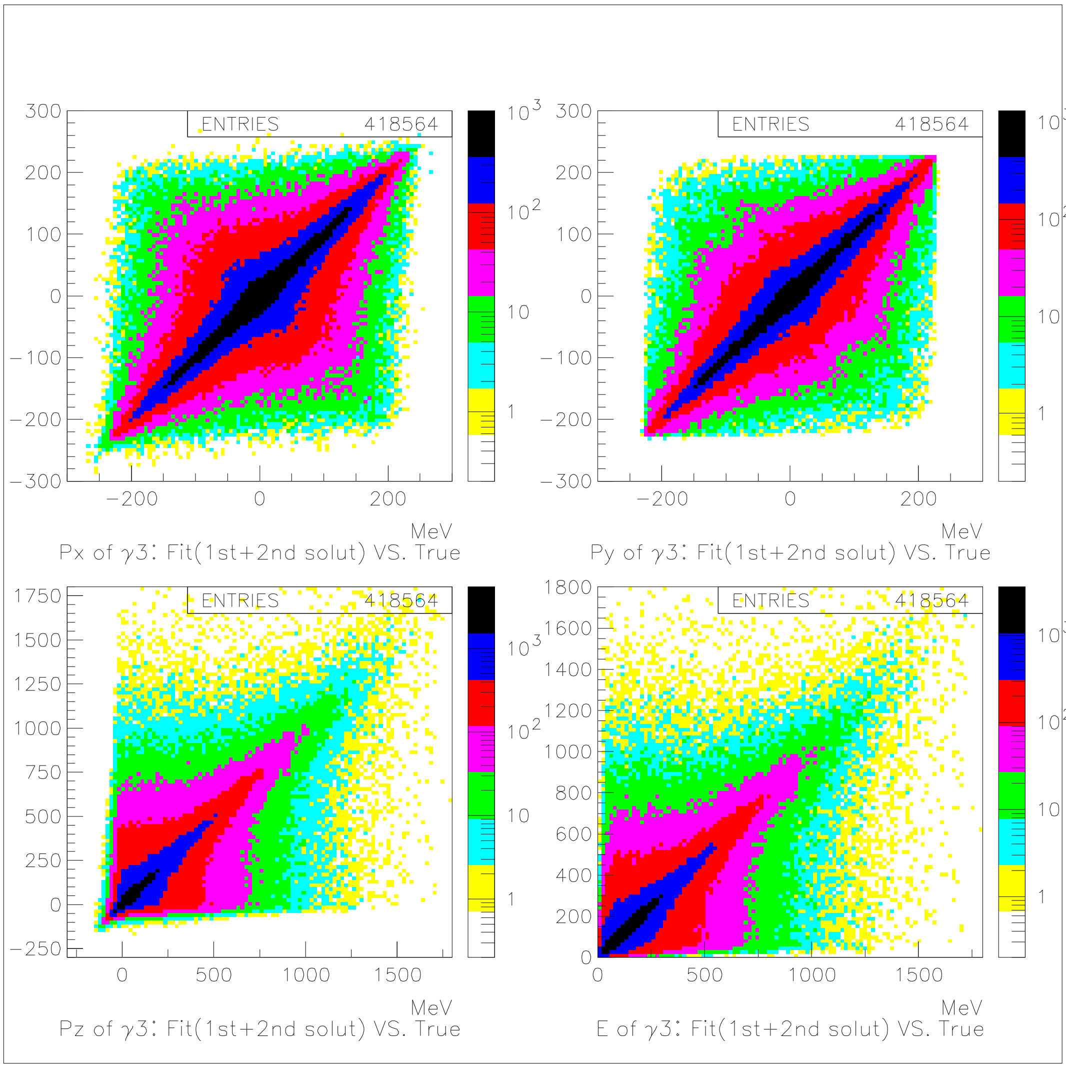

Figure 6: The fit results for the LAB 4-momentum of γ_3 versus the corresponding true values. Both of the 2 possible solutions are plotted.

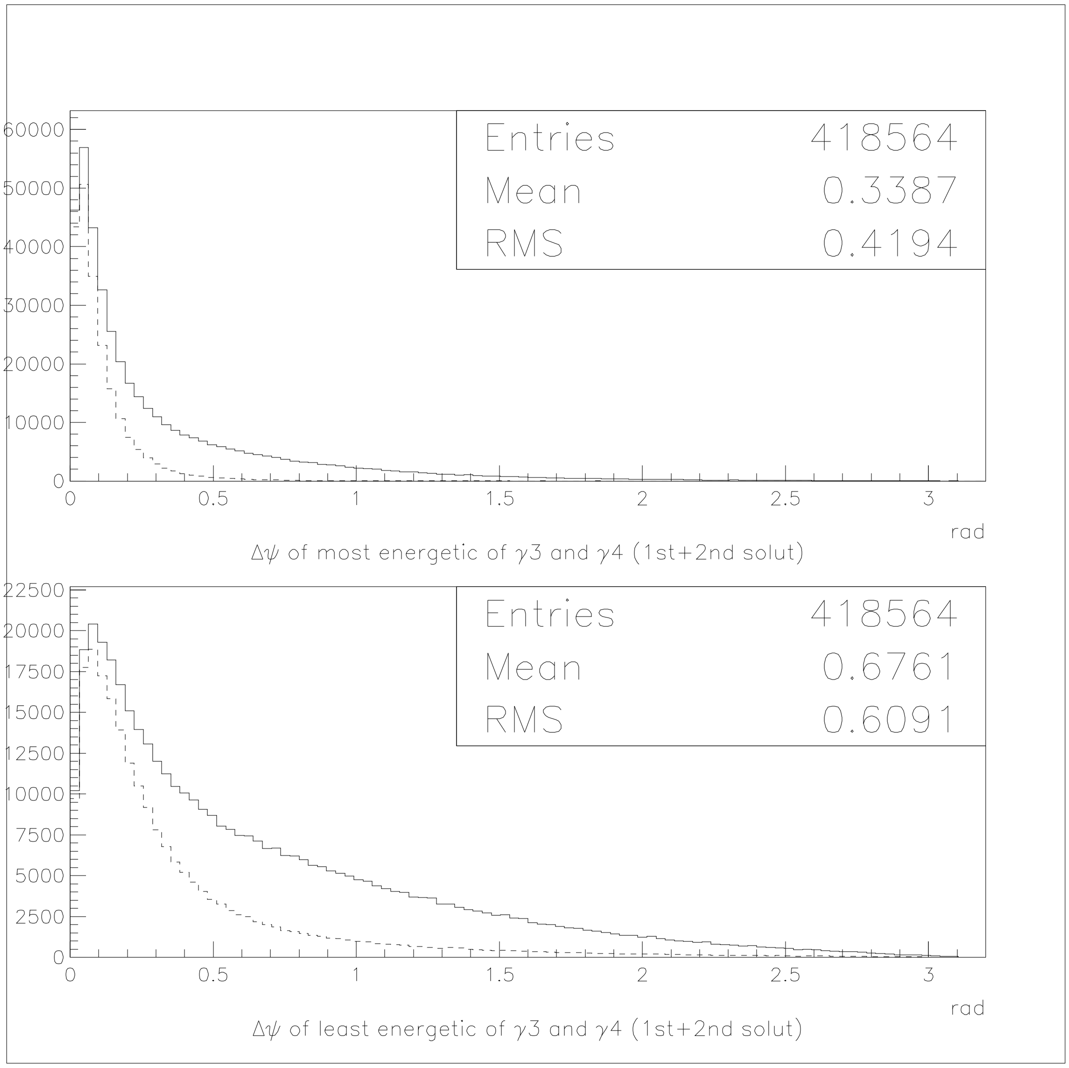

Figure 7: Top: the solid histogram represents the angle $\Delta\psi$ (see Eq. 13) between the predicted and true LAB direction of the most energetic of the undetected photons; both 1st and 2nd solutions are used. The dashed histogram represents the best one between the 1st and 2nd solutions. Bottom: as above but for the least energetic of the undetected photons.

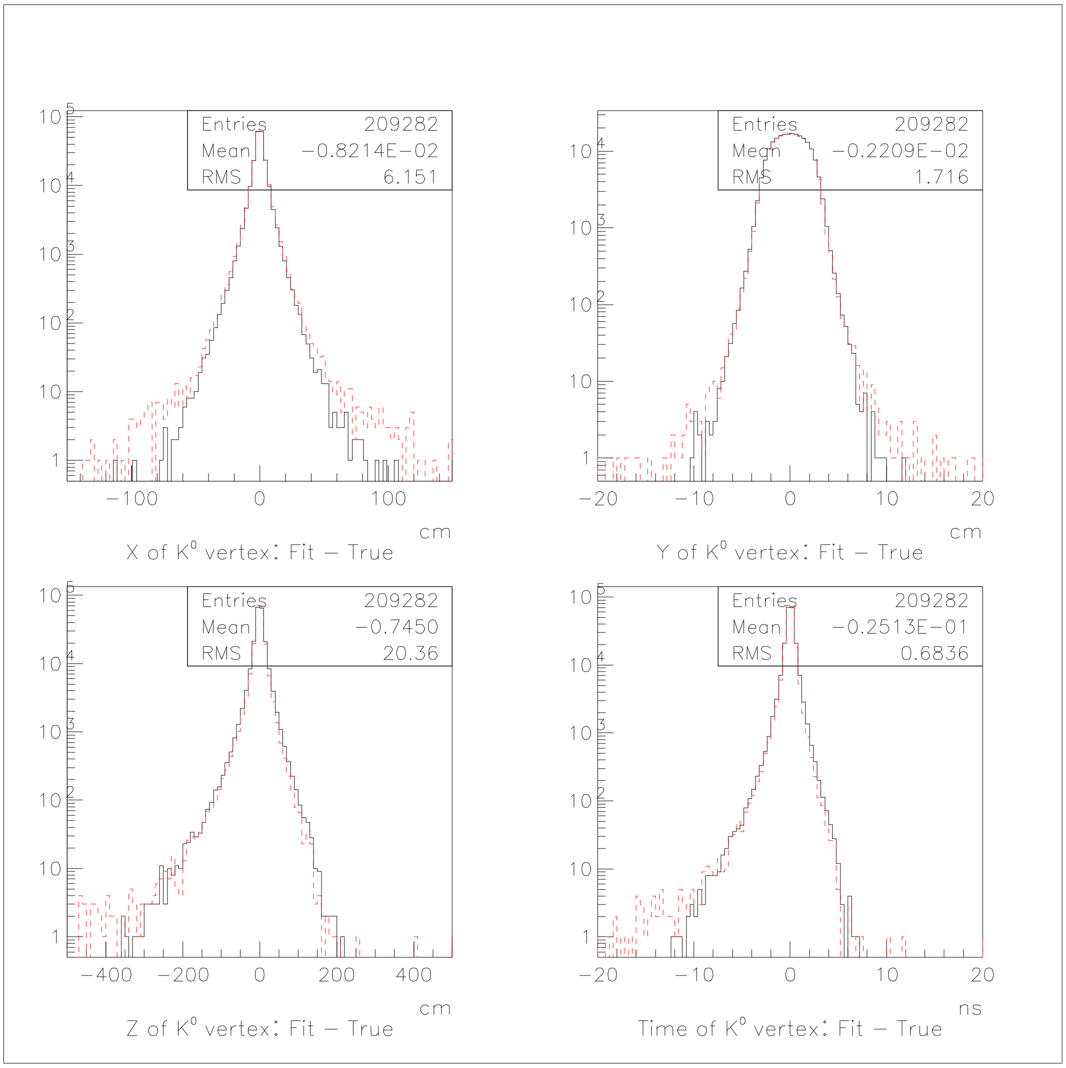

Figure 8: Solid histograms: the resolution of the kp2-odd fitter on the decay vertex of the K^0. (Since the 2 solutions of the kp2-odd fitter share the same K^0 decay vertex, the 2-fold ambiguity does not apply here.) Dashed histograms: the resolution of the $X \to \gamma_1\gamma_2$ fitter. (The y-position of the vertex is assumed to be within the y-dimension of the beam and is treated as a measured quantity by the fitters.)

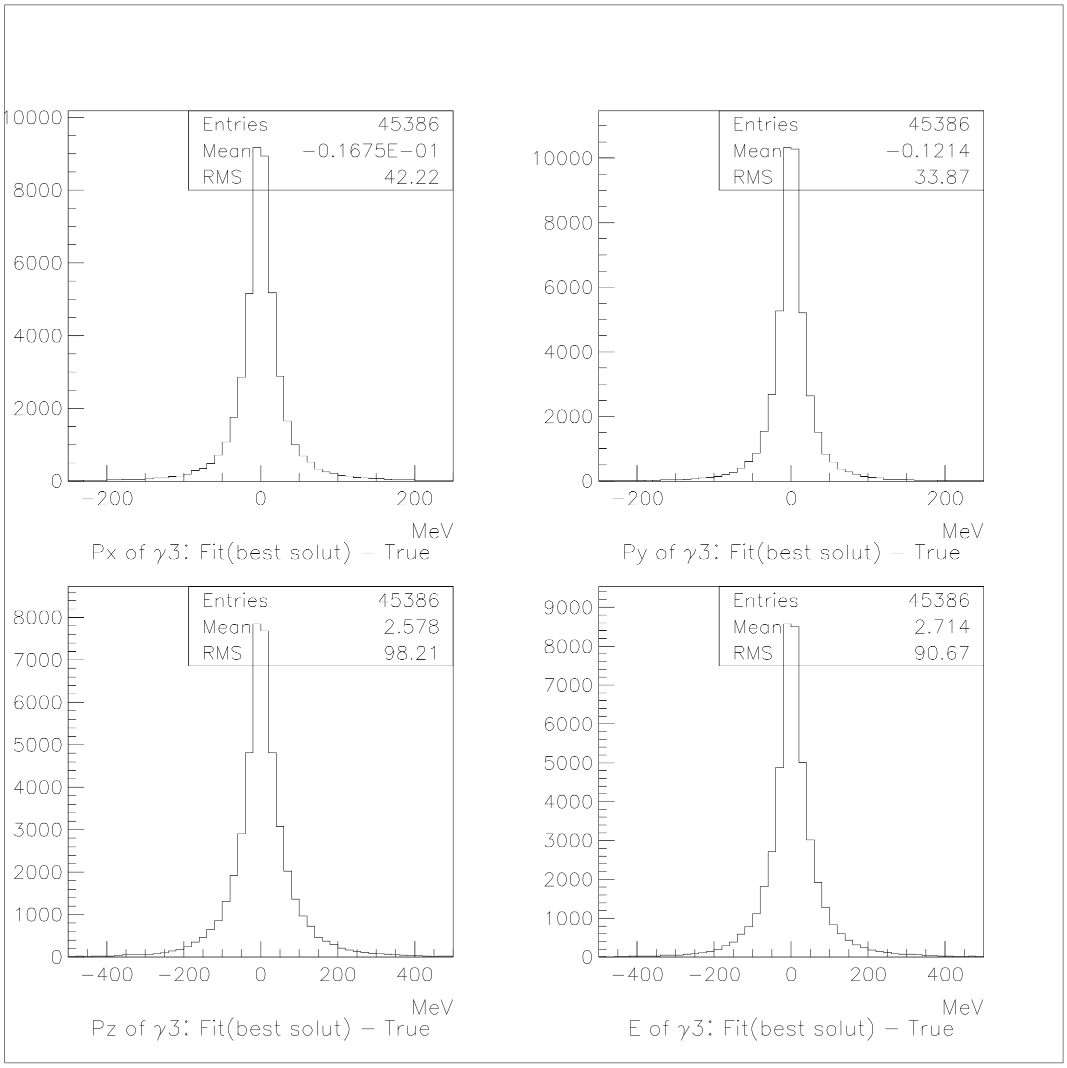

Figure 9: As the solid histogram in Fig. 3, but only for events with no analytical solutions. The kp2-odd fitter resolution for these events, which constitute about 22% of the sample of events with a converging fit, is about 15% worse than the resolution for the full sample.

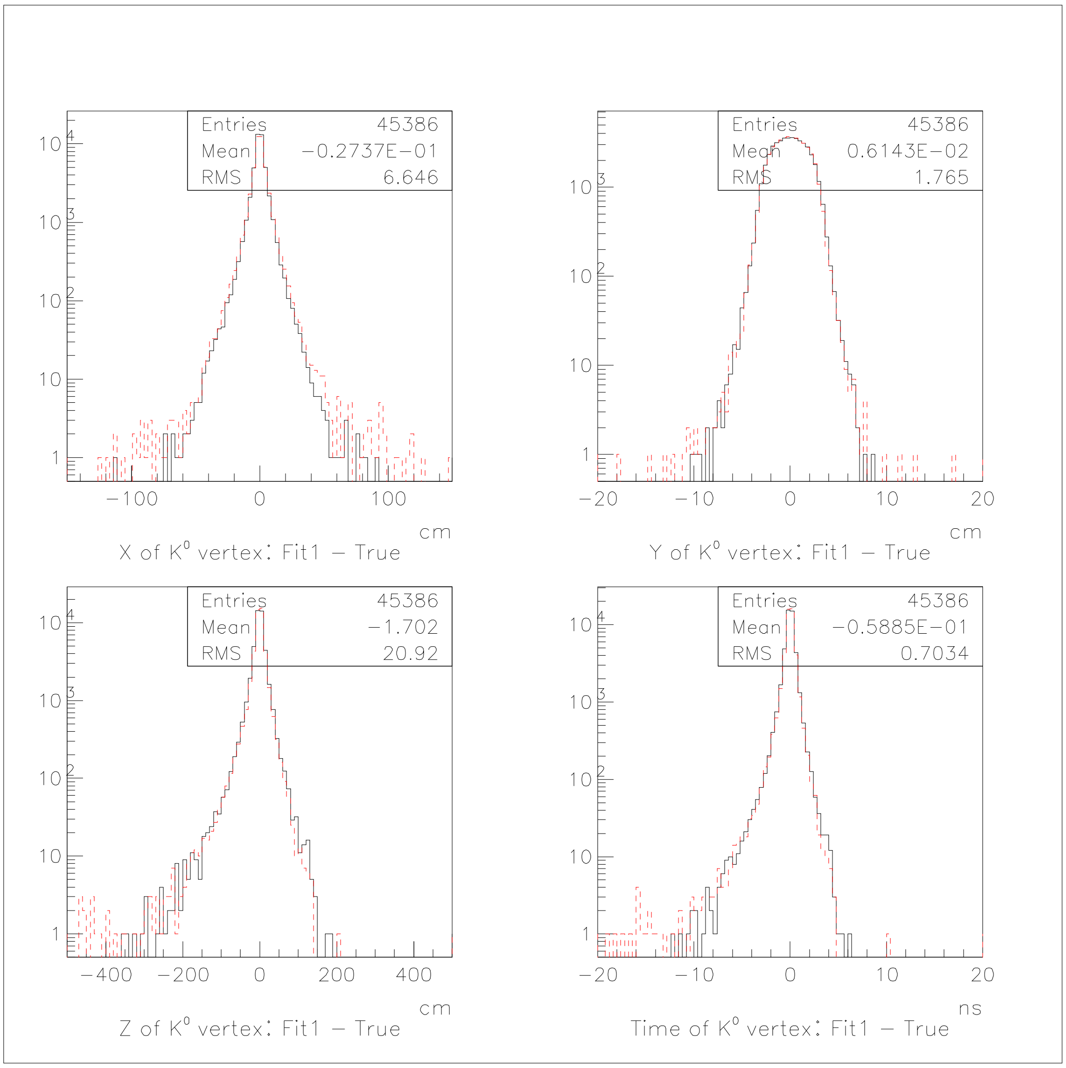

Figure 10: As in Fig. 8, but only for events with no analytical solutions. The kp2-odd fitter resolution on the K^0 vertex for these events is similar to the resolution for the full sample.

4 Comparing the results of the kp2-odd fitter for events kp2-odd, kpnn, and kp2-even

In this section and the following plots, only those kp2-odd events that pass a standard kpnn selection are considered. In addition, comparisons are made with kp2-even and kpnn events that satisfy the same selection. The purpose is to investigate possible differences among the kp2-odd fit results for the 3 categories of events. The applied kpnn selection is the following:

- $|m_{\gamma_1,\gamma_2} - m_\pi| < 20$ MeV
- Successful fits to $X \rightarrow \gamma_1\gamma_2$ and $\pi^0 \rightarrow \gamma_1\gamma_2$
- χ^2 of fit to $X \rightarrow \gamma_1\gamma_2 < 100$
- Distance of closest approach (DOCA) < 60
- 1090 cm$< z_K <$1365 cm, where z_K is the z-position of the K^0 from the fit to $\pi^0 \rightarrow \gamma_1\gamma_2$
- Contour Cut (see FORTRAN code below)

```
x = log(RecEmiss(irec))
y = RecEPinCMS(irec) - 135.
y = y*y
LcutEmiss = .TRUE.
if (x.lt.5.5 .or. y.lt.1000. .or. y.gt.22000.) then
   LcutEmiss = .FALSE.
else
   if (x.lt.6.75.and.y.lt.27250.-x*2000.) then
      if (y.lt.9500.-x*1000.)   LcutEmiss = .FALSE.
      if (y.gt.-9600.+x*3200.)  LcutEmiss = .FALSE.
   endif
endif
```

Table 1 show the percentage of convergence of the kp2-odd fitter applied to kp2-odd, kp2-even and kpnn events. The table also gives the percentage of events for which analytical solutions to the kp2-odd kinematic problem exist.

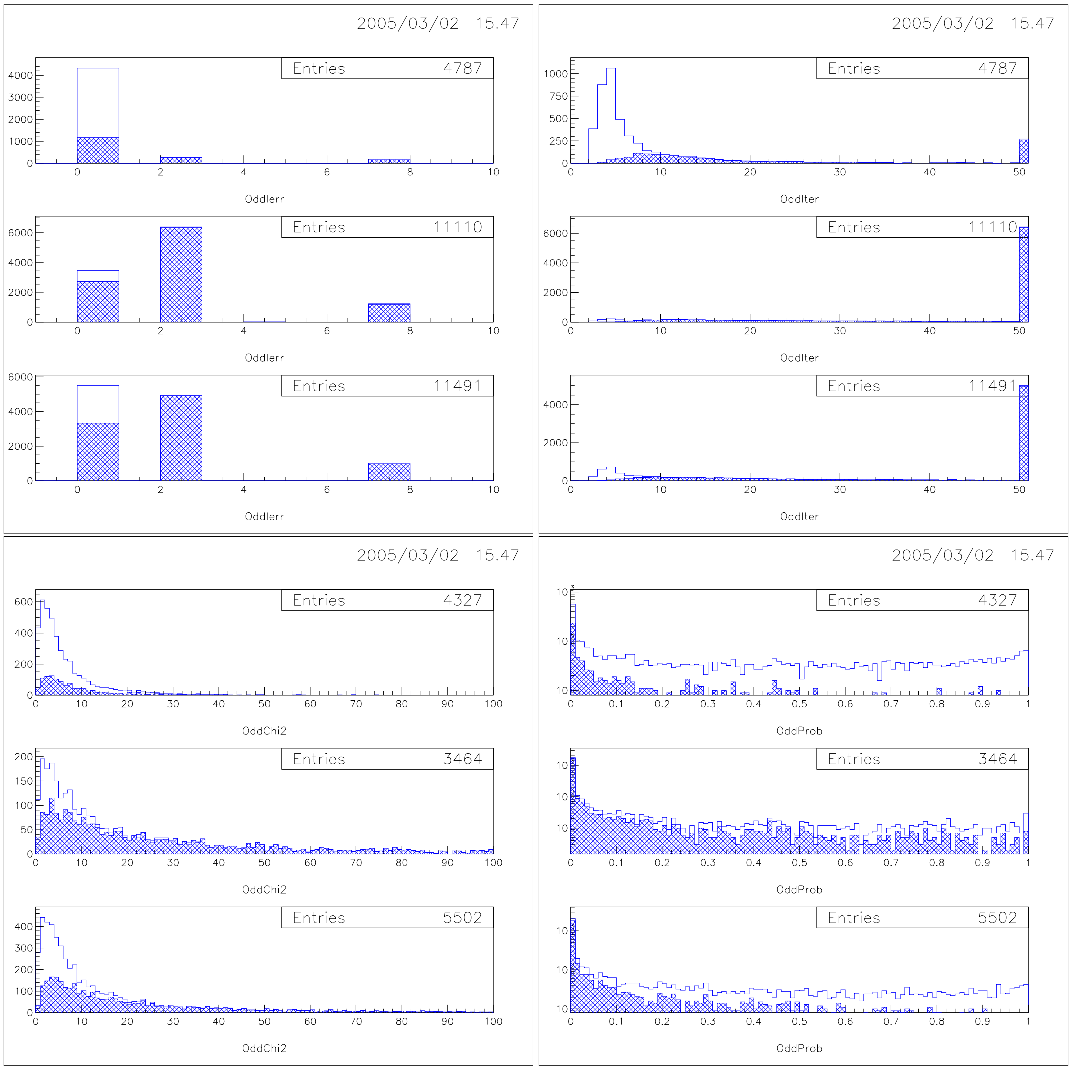

Figure 11: Top-left box: error code of kp2-odd fitter applied to kp2-odd (top), kp2-even (center) and kpnn (bottom) events that passed standard kpnn cuts; OddIerr = 0, 2 and 7 means normal convergence, exceeded maximum number of iterations and fit failure, respectively. The dark histograms show those events for which there was no analytical solution before performing the fit. Top-right box: number of kp2-odd fit iterations.
In the 2 bottom boxes, only events with a converging kp2-odd fit (OddIerr = 0) are considered. Bottom-left box: χ^2; the distribution is truncated at $\chi^2 = 100$. Bottom-right box: probability of χ^2.

Event type	Fit OK OddIerr=0	N. Iter>50 OddIerr=2	Failure OddIerr=7	Analytical Solutions
kp2-odd (all events)	90% (78%)	5% (4%)	5% (18%)	72%
kp2-odd (after kpnn sel.)	90% (73%)	6% (4%)	4% (14%)	67%
kp2-even (after kpnn sel.)	31% (21%)	58% (0.5%)	11% (4%)	7%
kpnn (after kpnn sel.)	48% (39%)	43% (0.7%)	9% (5%)	20%

Table 1: Percentage of events for which the kp2-odd fitter converges or fails. OddIerr = 0, 2 and 7 means normal convergence, exceeded maximum number of iterations and fit failure, respectively. For each considered OddIerr, the number in brackets gives the percentage of events for which analytical solutions of the kp2-odd kinematic problem exist. The last column gives the total percentage of events with existing analytical solutions.

Fig. 11 shows the kp2-odd fitter error code, number of iterations, χ^2 and probability of χ^2.

Fig.s 12, 13 and 14 show the distributions of $E^*_{\gamma_1} + E^*_{\gamma_2}$ VS $E^*_{\gamma_1} - E^*_{\gamma_2}$ for those events with a converging/failing kp2-odd fit and those with/without analytical solutions to the kp2-odd kinematic problem.

Some other quantities are explored below. The distance, in CM momentum space, between the 2 possible π^0 solutions is shown in Fig. 15. The prediction that the kp2-odd fitter makes for the LAB value of θ of the hypothesized undetected photons for kp2-odd, kp2-even and kpnn events is shown in Fig. 16.

A quantitative statement on whether the kp2-odd fit/reconstruction can improve the background rejection has not been reached yet and studies are still ongoing.

5 Acknowledgements

I would like to thank M. Marx, who is the original promoter of this study, D. Jaffe for his frequent help and suggestions, and D. Vavilov, who is the author of the routine named KINGPS.

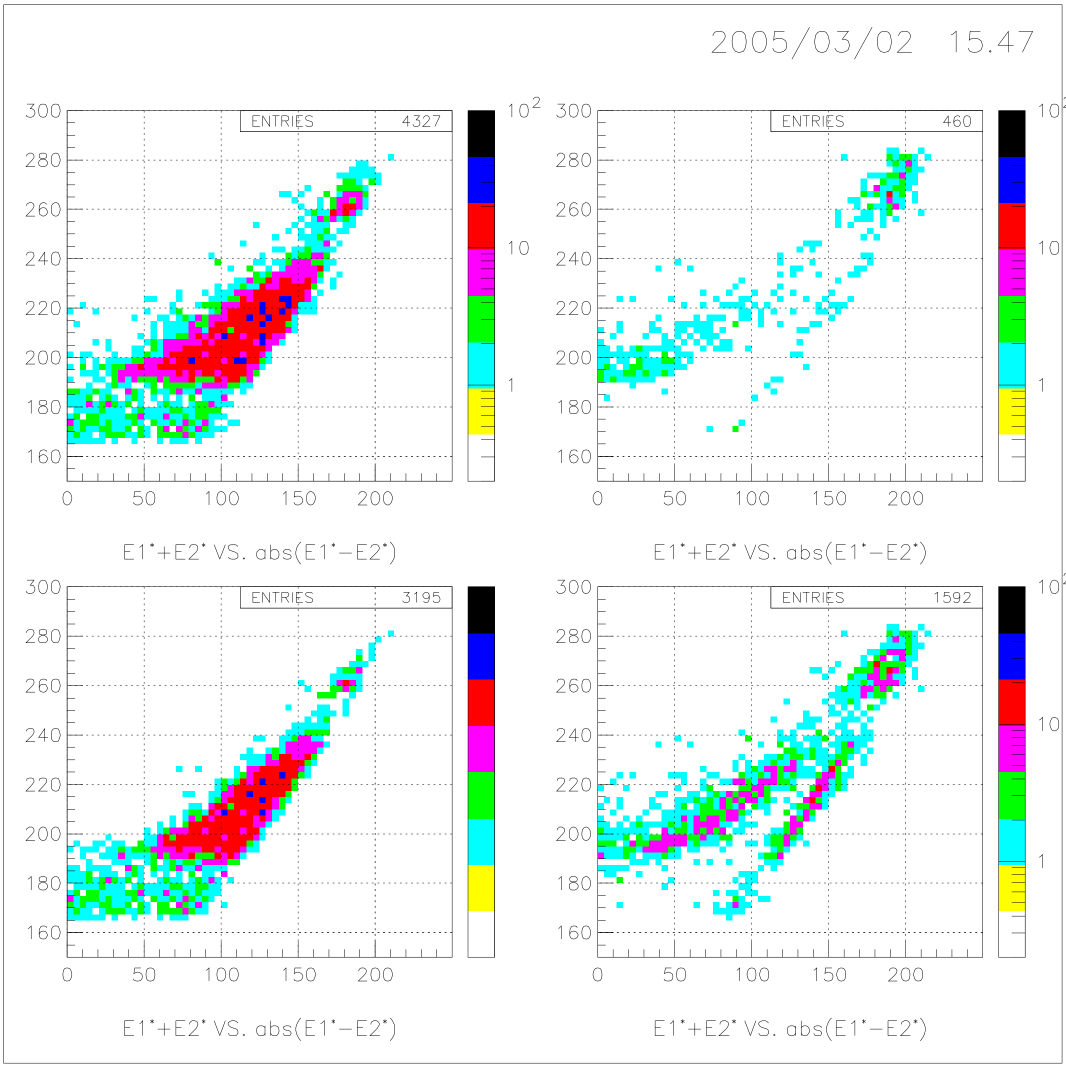

Figure 12: The $E^*_{\gamma_1} + E^*_{\gamma_2}$ VS $E^*_{\gamma_1} - E^*_{\gamma_2}$ distribution of kp2-odd events after kpnn selection. (The values used for $E^*_{\gamma_1}$ and $E^*_{\gamma_2}$ are the outputs of the fit to $\pi^0 \to \gamma_1\gamma_2$.)
Top left (right): events with a converging (failing) kp2-odd fit.
Bottom left (right): events with (without) analytical solutions to the kp2-odd kinematic problem.

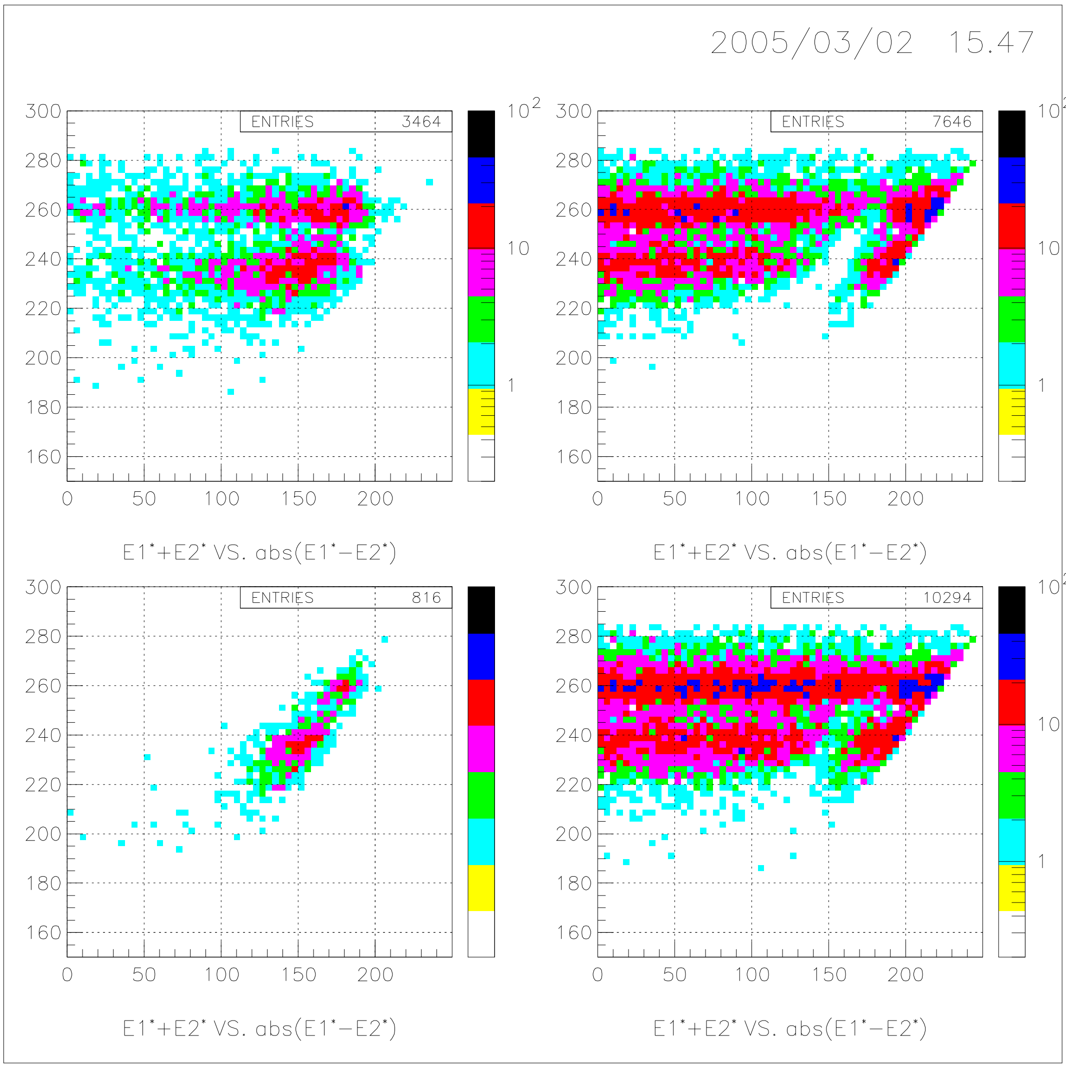

Figure 13: As in Fig. 12, but for kp2-even events.

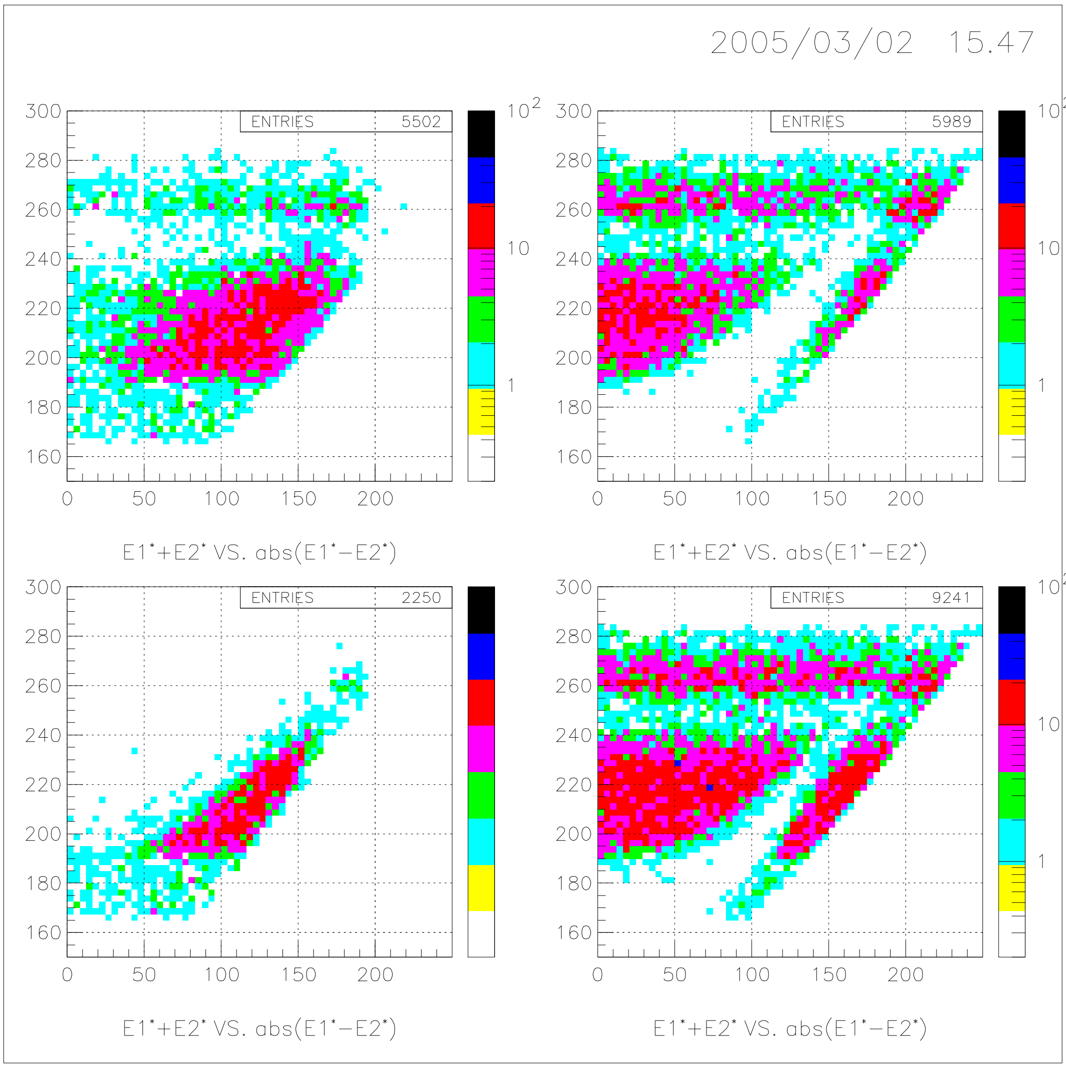

Figure 14: As in Fig. 12, but for kpnn events.

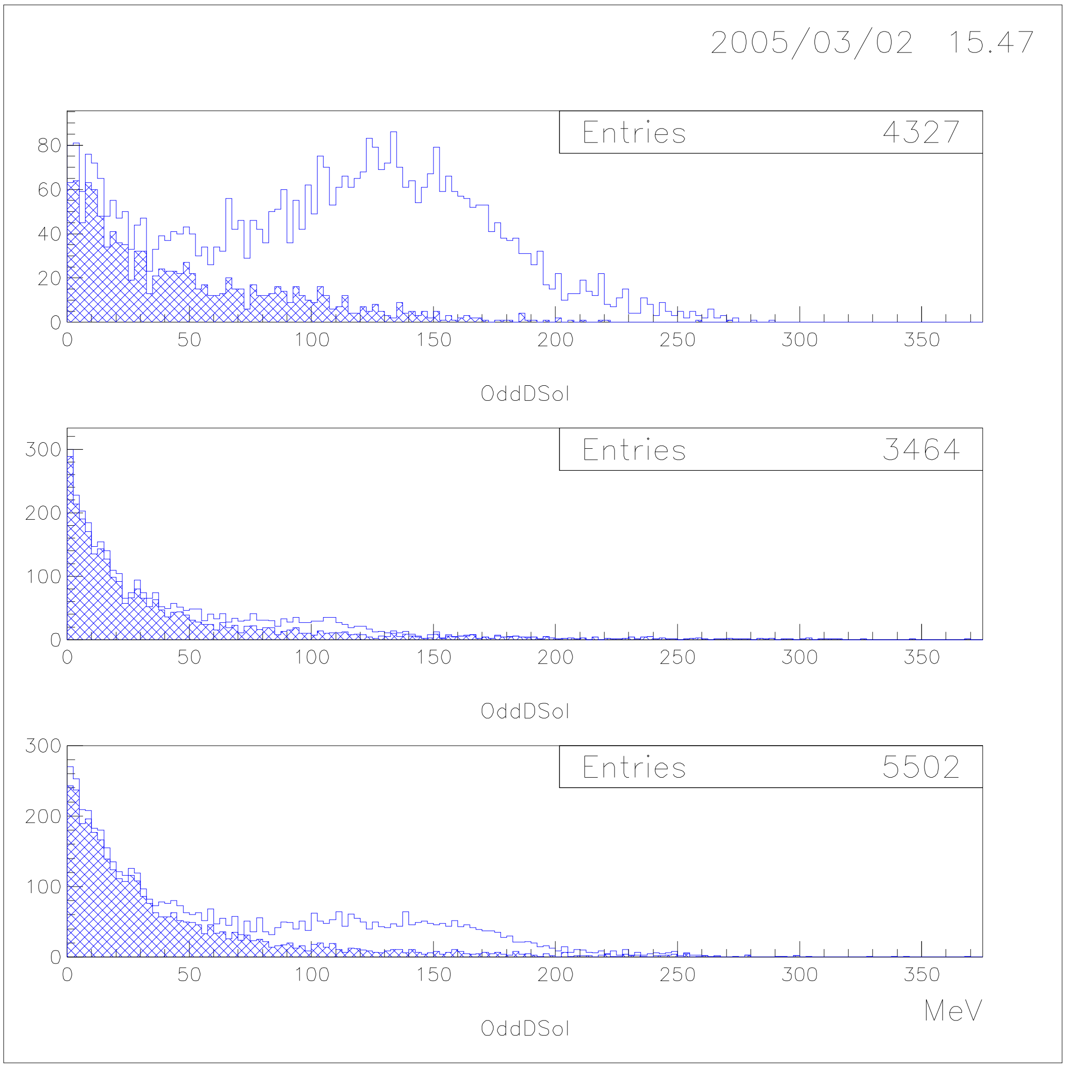

Figure 15: Distance in CM momentum space between the 2 possible solutions for a π^0, i.e. $|\vec{P}_\pi(\mathrm{2nd\ solut.}) - \vec{P}_\pi(\mathrm{1st\ solut.})|$. Top, center and bottom plots represent kp2-odd, kp2-even and kpnn events, respectively. The dark histograms represent those events for which there was no analytical solution before performing the fit.

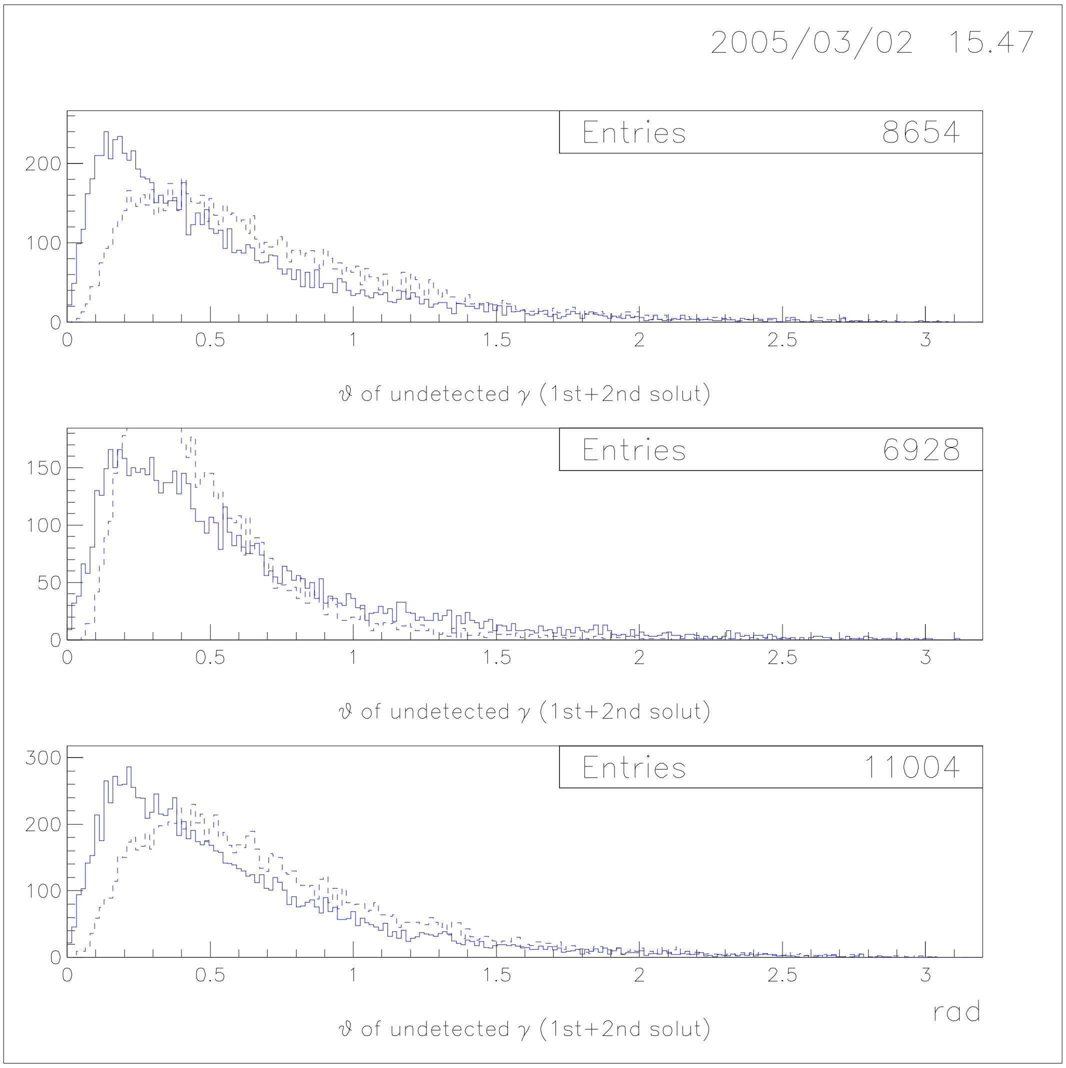

Figure 16: The predicted LAB value of θ of the hypothesized undetected photons for kp2-odd (top), kp2-even (center) and kpnn (bottom) events. In each plot, the solid histogram represents the undetected photon associated with the most energetic (in LAB) of the measured photons γ_1 and γ_2; both 1st and 2nd solutions are plotted. (We cannot define, using the fit results, a most energetic between the undetected photons γ_3 and γ_4, as there are 2 different solutions with different LAB energies.) The dashed histogram represents the undetected photon associated with the least energetic photon between γ_1 and γ_2.